6688 *Macromolecules* **2009**, *42*, 6688–6697
DOI: 10.1021/ma900889d

Macromolecules
ARTICLE

Ordered Arrays of PS-*b*-P4VP Micelles by Fusion and Fission Process upon Solvent Annealing

Tae Hee Kim,[†] June Huh,[†] Jiyoung Hwang,[†] Ho-Cheol Kim,[‡] Seung Hyun Kim,[§] Beong-Hyeok Sohn,[∥] and Cheolmin Park*,[†]

[†]*Department of Materials Science and Engineering, Yonsei University, Seoul 120-749, Korea,* [‡]*IBM Research Division, Almaden Research Center, 650 Harry Road, San Jose, California 95120,* [§]*Division of Nano-Systems Engineering, Inha University, Incheon 402-751, Korea, and* [∥]*Department of Chemistry, Seoul National University, Seoul, Korea*

Received April 22, 2009; Revised Manuscript Received July 16, 2009

ABSTRACT: We systematically investigate the morphological evolution of monolayered micelle films of poly(styrene-*block*-4vinylpyridine) (PS-*b*-P4VP) copolymers with different molecular weight and compositions upon tetrahydrofuran (THF) solvent annealing. Despite the final ordered arrays of the spherical micelles achieved with long-range order for all block copolymers after 3 h of solvent annealing, two different ordering mechanisms are observed. Solvent annealing of as-cast spherical micelles of a PS-*b*-P4VP copolymer with a PS corona block shorter than ~20 000 g/mol gives rise to cylindrical micelles by intermicelle fusion, which subsequently divide themselves into spherical micelles with long-range ordering by fission. A long-range order of spherical PS-*b*-P4VP micelles with long PS corona of ~50 000 g/mol occurs just by rearrangement of the micelles without fusion and fission of the initial micelles during solvent annealing. The $HAuCl_4$ salt preferentially loaded in the P4VP cores strongly ties P4VP chains together and consequently delays the micelle fusion, leading to a poor ordering of the micelles, even after long-time solvent annealing. We also demonstrate a technologically useful way in which one chooses ordered arrays of either cylindrical or spherical micelles confined into a topographic prepattern by controlling solvent annealing kinetics.

Introduction

Nanostructures based on the self-assembly of synthetic block copolymers have been of great interest because of their facile, simple, and thus cost-effective fabrication with many emerging applications in nanotechnology including nanolithography, photonic band gap materials, drug carriers, and templates for harvesting metal or inorganic materials.[1,2] In particular, amphiphilic block copolymers, similar to low-molecular-weight surfactants, aggregate to form micelles in a preferential solvent to one of blocks above a critical micelle concentration.[3] In most cases, spherical block copolymer micelles in a solvent are characterized with the insoluble blocks collapsing together to form the core and the soluble blocks forming the corona, which extends into the solvent environment.[4]

The building units of spherical micelles easily assemble themselves to form highly packed structures owing to their size uniformity and excellent kinetic stability for various aforementioned solid-state applications. The pseudohexagonal arrays of micelles are deposited upon casting spherical micelles into an ultrathin film on a flat solid substrate.[5] Langmuir−Blodgett,[6] dip-coating,[7] and spin-coating[8] methods have successfully fabricated ultrathin films of block copolymer micelles. Further benefit of the block copolymer micelles over conventional organic or inorganic colloids lies in the fact that the micelles are conveniently coupled to various external fields such as temperature,[9] shear,[10] geometrical confinement known as graphoepitaxy,[11] and solvent vapor,[12] leading to near-defect-free ordered structures, which are obviously more desirable for realization of the potential application of pattern masks for nanolithography.

Thermal annealing of an as-cast micelle film has been a common way for improving the ordering of the hexagonal structure but is considered to be less effective because of its time requirement of longer than at least 10 h. The recent work by Register et al.[10,13] has demonstrated that static shear was very useful for ordering monolayered spherical microdomains of a block copolymer over a large area. The quantized spatial confinement of either spherical domains or micelles on topographical periodic prepattern has turned out to be very beneficial for controlling the orientation and registry of the assembled structures, in particular, combined with thermal annealing.[14,15]

Utilization of solvent for controlling micelle assembly can be categorized into two main approaches. One is to control the solvent evaporation rate in forming a film from the micelles dispersed in solution[15,16] and the other is to expose solvent vapor or a mixture of solvent vapors to an as-cast thin micelle film for a certain period of time as referred to solvent annealing. One can easily notice that most of inorganic and polymeric colloids have been assembled into ordered structures by the first method in which the gradient of the solvent evaporation rate arising from the meniscus formed at the air−solution substrate interface imparts directional solvent evaporation, leading to highly ordered assembled structures.[17−19] A similar approach was successfully employed in the ordering of block copolymer micelles.

The solvent annealing has been one of the most effective ways for fabricating not only highly ordered micelle structures but also vertically ordered lamellar and cylindrical microdomains despite less understanding of the mechanism of structural ordering. The original work by Kim et al.[20] revealed that neutral environment by benzene vapor successfully induced large area orientation of

*Corresponding author. Tel: +82-2-2123-2833. Fax: +82-2-312-5375. E-mail: cmpark@yonsei.ac.kr.

 Published on Web 08/06/2009

cylindrical poly(styrene-*block*-ethylene oxide) microdomains aligned perpendicular to the substrate. Many other groups have reported the controlled block copolymer structures under solvent vapor exposure with different block copolymers and solvents.[21−30] Block copolymer micelle films with long-range order have also been produced by solvent annealing. Large area ordering of monolayered PS-*b*-P4VP micelles was achieved by the exposure of THF solvent vapor for 30 min.[12] A well-ordered PS-*b*-P4VP micelle film developed by solvent annealing was utilized as an etching mask for nanopatterned porous alumina surface.[31] In addition, hexagonally packed spherical PS-*b*-P4VP micelles were used for fabricating highly ordered porous nanostructures by solvent annealing with cosolvent vapor of THF and toluene.[32]

Furthermore, different from thermal annealing of a micelle film at the temperature below order−disorder transition temperature, during which block copolymer microdomains thermodynamically determined are maintained, solvent annealing can provide various kinetic pathways that involve different microstructures because of the preferential interaction of the solvent to one of blocks.[33] At the same time, it offers a useful way with which we can fabricate technologically useful microstructures kinetically controlled as long as we understand the structural evolution route with time during solvent annealing. It is, however, unfortunate that only a few works have dealt with the kinetics of ordering process of block copolymer film during solvent annealing.[34−36]

In this contribution, we systematically investigate the morphological evolution of a thin PS-*b*-P4VP micelle film upon THF solvent annealing. We have observed two different kinetic pathways to reach ordered arrays of spherical micelles upon 3 h solvent annealing, depending on relative corona block length. As-cast spherical micelles of a PS-*b*-P4VP with long corona PS blocks refine their position and registry into an ordered structure with solvent vapor. More interestingly, when a PS-*b*-P4VP with corona blocks shorter than ∼20 000 g/mol is employed, well-defined spherical micelle arrays with long-range order are achieved through the fusion and fission process in which cylindrical micelles formed by the fusion of the initial micelles are transformed again into spherical micelles with excellent ordering. We controlled the orientation driven by the fusion and fission process by incorporating $HAuCl_4$ salt in the P4VP cores that strongly bind P4VP block together and thus significantly hinder the fusion of the initial spherical micelles into cylindrical micelles.

Experimental Part

Materials. All amphiphilic poly(styrene-*block*-4-vinyl pyridine) (PS-*b*-P4VP) copolymers were purchased from Polymer Source (Doval, Canada). Various PS-*b*-P4VP copolymers with lamellar, cylindrical, and spherical microstructures in bulk state were employed with different block lengths. The characteristics of the block copolymers are shown in Table 1.

Hydrogen tetrachloroaurate(III) trihydrate ($HAuCl_4 \cdot 3H_2O$) was purchased from Sigma-Aldrich (99.99%). $HAuCl_4 \cdot 3H_2O$ (0.01 to 1 equiv) with respect to P4VP block was dissolved with PS-*b*-P4VP micelles in toluene. The $HAuCl_4 \cdot 3H_2O$ was selectively loaded in P4VP cores to restrain P4VP cores for controlling the fusion of spherical micelles.

Film Preparation. A PS-*b*-P4VP block copolymer was dissolved in toluene with 0.5 wt % at 80 °C for 30 min. Because of the preferential interaction of toluene to PS block, spherical micelles with PS corona and P4VP core are readily formed. Thin monolayered PS-*b*-P4VP films were prepared by spin coating at 7000 rpm on Si wafer (SPIN 1200 Midas-system, Korea). The thin films were subsequently placed in the chamber with tetrahydrofuran (THF) vapor for different solvent annealing time. The environment outside the chamber was maintained at 25 °C and 20% humidity. The samples treated with solvent vapor were immediately taken out of the jar and dried at room temperature to minimize further structural evolution. Two solvent annealing protocols were employed to investigate the evolution of microstructures of micelle films. In the first case, a sample treated with solvent for a certain period of time was taken out for structural investigation, and subsequently, the same sample was again treated with solvent vapor for an additional time period and examined. In the other case, we prepared several as-cast micelle films and began to anneal them with THF at once. Each sample was taken out and examined after the corresponding solvent annealing time period. We found that both protocols gave rise to the similar structural evolution of the micelle films. A monolayered film was also prepared on a topographic prepattern by spin coating and subsequently solvent-treated for 3 h for better control of the block copolymer structures.

Prepatterns. Topographic Si prepatterns with periodic lines and circular dents were fabricated by conventional optical lithography technique using 193 nm photoresist and subsequent etching with CF_4 plasma. The line pattern has the width of trench and mesa of 340 and 580 nm, respectively, and the circular pattern consists of the circular dents of 250 nm in radius arrayed with *p*4*mm* symmetry. The depth of line trenches and circular dents is ∼45 nm, and the contact angles of water on the prepatterns were all ∼43°.

Characterization. The size of block copolymer micelles in solution was characterized by dynamic light scattering (DLS) (Malvern CGS-3) with $\lambda = 633.2$ nm, and the scattering angle was 90°. Intensity autocorrelation functions, $g(2)(t)$, were recorded at room temperature. Correlation function, $g(1)(t)^2$, was related by $g(2)(t) - 1 = g(1)(t)^2$ with the minimum deviation from the ideal correlation and was plotted as a function of time. Inverse Laplace transformations were performed using the constrained regularization calculation program REPES to obtain the distribution of relaxation times, $G(\Gamma)$, where Γ is relaxation time. In addition, the size and nanostructures of the block copolymer micelles on Si substrate were analyzed with atomic force microscope (AFM) in tapping mode (Nanoscope IVa, Digital Instrument). The dewetting behavior of the monolayered micelle films was observed during solvent annealing by optical microscope (OM) (Olympus BX 51M) in bright field. We measured X-ray photoelectron spectra (XPS) with SIGMA PROBE (ThermoVG, U.K.) at room temperature by using a monochromatic Al Kα X-ray source at 12 kV and 100 W. The sample analysis chamber of the XPS instrument was maintained at a pressure of 1.8×10^{-9} mb. Grazing-incidence small angle

Table 1. Characteristics of the PS-*b*-P4VP Copolymers Employed

samples	total M_w (kg/mol)	M_{wPS} (kg/mol)	total M_w/M_n	ϕ_{PS}	ϕ_{P4VP}	bulk morphology	D_H (nm) in solution[a]	d (nm) on substrate (as-cast)[b]	d (nm) after solvent annealing[b]
PS-*b*-P4VP1	68.5	47.6	1.14	0.71	0.29	cylinders	114	31	24
PS-*b*-P4VP2	37	20	1.08	0.55	0.45	lamellae	61.4	25	20
PS-*b*-P4VP3	23.8	12	1.04	0.52	0.48	lamellae	47.2	20	15
PS-*b*-P4VP4	39	20	1.09	0.53	0.47	lamellae	75.4	31	22
PS-*b*-P4VP5	33.5	16.5	1.09	0.51	0.49	lamellae		30	26
PS-*b*-P4VP6	29.6	10.4	1.27	0.36	0.64	cylinders	36.8	17	15

[a] Averaged hydrodynamic diameter of spherical micelles measured in solution by DLS. [b] Averaged diameter of spherical micelles evaluated on a substrate by AFM images.

X-ray scattering (GISAXS) was performed to characterize the structure of block copolymer thin films on the 4C2 beamline at the Pohang Accelerator Laboratory in Korea. The measurements were performed with monochromatized X-rays ($\lambda = 0.1380$ nm) having grazing incident angles ranging from 0.09 to 0.20°, and the scattered intensity was recorded by SCX (4300-165/2 CCD detector, Princeton Instruments).

Results and Discussion

All PS-*b*-P4VP copolymers employed in this work are assembled into spherical micelles with highly swollen PS corona blocks in toluene. The size of the micelles in solution was obtained and is listed in Table 1 by DLS, where inverse Laplace transformations performed using the constrained regularization calculation offered the distribution of relaxation times, which reflects the size distribution of the micelles. The diameter of micelles mainly depends on the aggregation numbers affected by the chemical structure of a block copolymer. In general, the aggregation number for an amphiphilic block copolymer is characterized by $Z = Z_0(N_A{}^{\alpha}N_B{}^{-\beta})$, where N_A and N_B are the degrees of polymerization of the insoluble and soluble blocks, respectively, and Z_0 is related to thermodynamic quantities such as an interaction parameter and a local packing parameter.[37] The experimental values for PS-*b*-P4VP/toluene solution were reported to be $\alpha = 1.93$, $\beta = 0.79$, and Z_0 of 1.66.[37] The core radii of PS-*b*-P4VP micelles with different molecular weights in Table 1 are qualitatively matched with the theoretical values.

The tapping mode AFM images in Figure 1a,b show the representative monolayered PS-*b*-P4VP1 and PS-*b*-P4VP3 micelles spin coated on Si substrates, respectively. The hydrodynamic diameter of PS-*b*-P4VP1 micelles measured by DLS was approximately 114 nm in solution. Because the swollen PS coronas in toluene were collapsed and vitrified during spin coating by rapid solvent evaporation, the diameter of the micelles and the center-to-center distance of two micelles become approximately 30 and 50 nm in the monolayer, respectively (Figure 1a). From the similar reason for PS-*b*-P4VP1 micelles with the higher molecular weight, the diameter of PS-*b*-P4VP3 micelle core and the center-to-center distance was approximately 20 and 30 nm, respectively as shown in Figure 1b. For the center-to-center distance between micelles, both the length of the corona chain proportional to N_B and the volume of core regions, $4\Pi R_c{}^3/3 = ZN_A v_A$, are crucial, where R_c and v_A are the radius of the micelle core and the molar volume of core monomers, respectively.[38] Because the aggregation number and the radius of cores increase with the degree of polymerization of core blocks, we can easily expect that the core size of PS-*b*-P4VP1 micelles is larger than that of PS-*b*-P4VP3.

Solvent annealing of both monolayered PS-*b*-P4VP1 and PS-*b*-P4VP3 micelle thin films with THF vapor for 3 h gave rise to long-range hexagonal ordering of the block copolymer microdomains, as shown in Figure 1c,d, respectively. THF is a good solvent for P4VP with a molecular weight of less than ~4 kg/mol. For the PS-*b*-P4VP copolymers studied in the current work, THF is slightly preferential to PS blocks. THF solvent, therefore, provided sufficient mobility of both copolymer chains and allowed the micelles in the film to assemble themselves into the highly ordered structure. Typical grains with near-defect-free ordered structure are ~3 μm in size for both block copolymers. In particular, our results with PS-*b*-P4VP1 micelles are very consistent with the work by Sohn et al., in which the same block copolymer was used for fabricating a well-ordered micelle structure with 20 min exposure of THF vapor.[12] The GISAXS images shown in the inset of Figure 1c,d exhibit strong first-order reflections along the q_y scattering vector. The reason for the observation of only the first-order reflection on our samples may be due to very thin films (~15 nm in thickness) mostly dewetted on the substrates after solvent annealing, as will be shown next. Extremely low contrast in our ultrathin dewet films renders it difficult to observe the higher-order reflections. A GISAXS pattern of an as-cast monolayered PS-*b*-P4VP3 film, in contrast, shows both the first and second reflections (Figure S1 in the Supporting Information). A 1D plot of the GISAXS results confirms the pseudohexagonal packing of the spherical micelles with the relative peak positions of high-order reflections with respect to the first peak position (q_n/q_1), yielding the expected values of 1 and $\sqrt{3}$. We tried hard to observe the higher-order reflections on a solvent annealed film, but the attempt has been unsuccessful. The $(10\bar{1}0)$ plane distances of PS-*b*-P4VP1 and PS-*b*-P4VP3 obtained from $2\pi/q_1$ are approximately 27 and 16 nm, which is consistent with AFM results.

Different from solvent annealing with a neutral solvent to both blocks, which locates both blocks at the polymer−solvent interface and thus results in ordered lamellar or cylindrical microdomains aligned perpendicular to the substrate, solvent annealing with THF turned out to be useful for fabricating ordered spherical micelles of PS-*b*-P4VP copolymers with PS coronas covering the film because of its preferential interaction to PS block. The presence of PS blocks dominantly at the polymer−air interface upon solvent annealing was evidenced by XPS data shown in Figure 1e,f. As expected, XPS spectra obtained from the ordered structures of both PS-*b*-P4VP copolymers are almost identical to the characteristic 1s electron peak of carbon at ~283 eV. In particular, the absence of a peak at 397 eV arising from the 1s electron of nitrogen in the spectra implies that P4VP blocks rarely exist at the interface. Combined with XPS results, AFM images in Figure 1c,d suggest that the spherical micelles with PS coronas are highly assembled into a hexagonally ordered structure. In contrast, a thin micelle film of PS-*b*-P4VP3 treated with ethanol vapor clearly exhibits the electron emission peak at 397 eV, which indicates that P4VP blocks preferential to ethanol vapor are dominantly located at the polymer−air interface (Figure S2 in the Supporting Information). It should be also noted that the ordered micelle structures observed are not thermodynamically stable but kinetically driven. All block copolymers in Table 1 show a similar ordered structure of spherical micelles after 3 h of solvent annealing with THF. Next, the morphological evolution of the ordered micelle film is investigated as a function of solvent annealing time.

Prior to the investigation of the microstructural evolution of a thin micelle film, we first monitored thin film behavior upon solvent annealing using an OM. A monolayered micelle film of PS-*b*-P4VP3 with thickness of approximately 13 nm began to dewet on a Si substrate, even after 10 min of THF vapor treatment, as shown in Figure 2a. Unlike the dewetting morphology of a thin polymer film characterized by hole formation and growth driven by nucleation and growth process, the observed morphology exhibits a typical early and intermediate stage structure in spinodal decomposition in which polymer concentration is periodically fluctuated and spontaneously amplified in space.[39−41] In the case of the ultrathin film, the surface pattern becomes unstable through capillary waves at the fluid−air interface, leading to the modulated pattern that is reminiscent of spinodal decomposition. This spinodal dewetting causes the film to rupture into droplets in the late stage of the process, as evidenced by OM images of our sample captured after long-time solvent annealing (Figure 2).

For a thin PS film on a Si substrate with a native oxide layer, spinodal dewetting occurs significantly, depending on both PS and oxide layer thickness upon thermal annealing.[42] The situation becomes more complicated in our system containing structured block copolymer micelles and a preferential solvent vapor. The PS blocks first contact on native oxide surface because the micelles with PS coronas in toluene were directly spin coated on

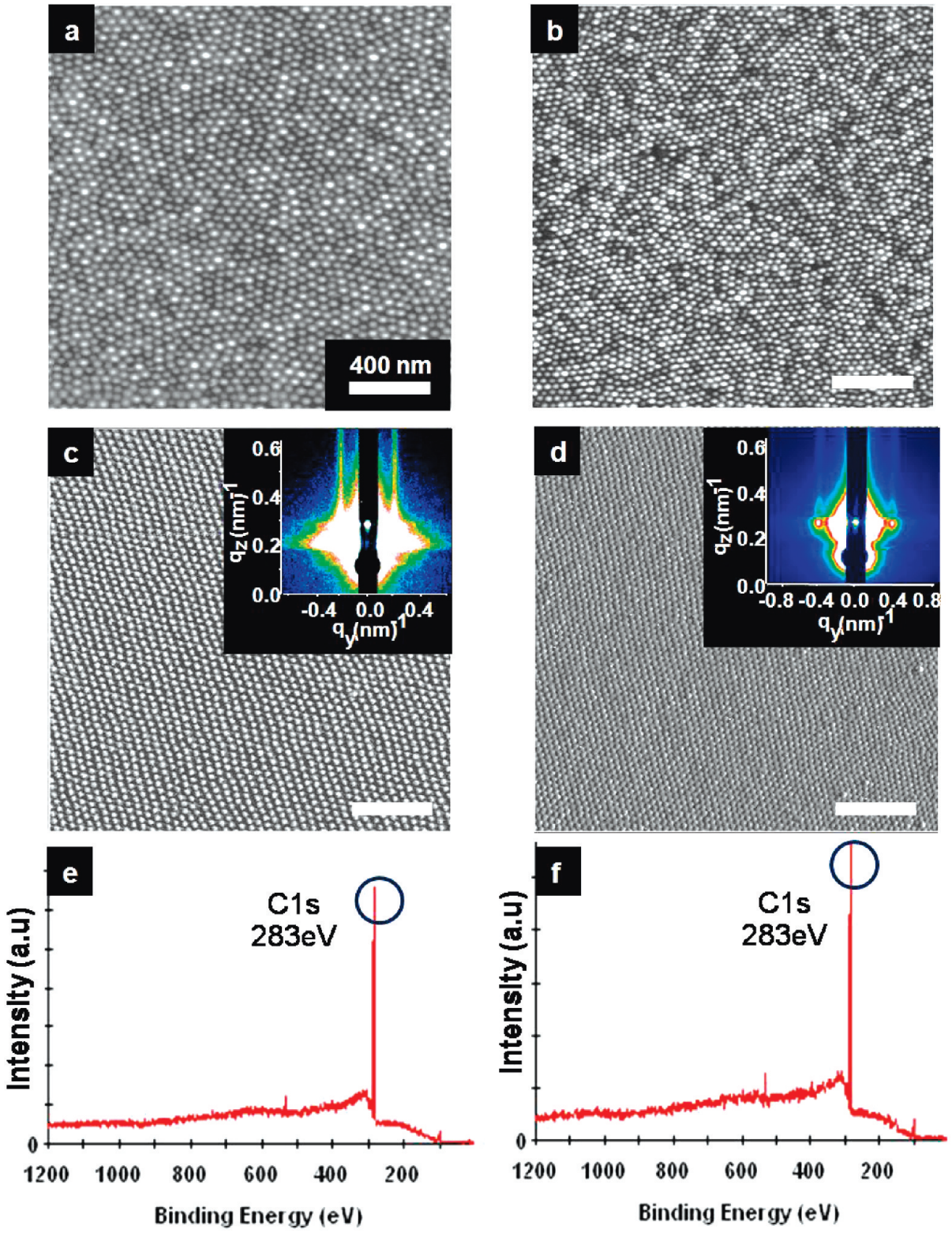

Figure 1. (a,b) TM-AFM images in height and (c,d) phase contrast of (a,c) monolayered PS-*b*-P4VP1 and (b,d) PS-*b*-P4VP3 micelle thin films. As-cast thin micelle films of (a) PS-*b*-P4VP1 and (b) PS-*b*-P4VP3 are transformed into well-ordered spherical micelle arrays (c and d) upon solvent annealing with THF vapor for 3 h, respectively. The insets of parts c and d correspond to 2D GISAXS patterns showing the strong first-order reflections of the hexagonally ordered spherical micelles of PS-*b*-P4VP1 and PS-*b*-P4VP3, respectively. (e,f) XPS spectra of solvent annealed PS-*b*-P4VP1 and PS-*b*-P4VP3 film for 3 h.

the substrate. It is known that the PS coronas in contact with the surface are severely collapsed during film formation and form very thin layers of approximately 5 nm in thickness, above which P4VP cores are located. One can speculate that the thin PS layer drives spinodal dewetting of the entire film when it becomes highly mobile with THF vapor preferential to PS blocks in the early stage of solvent annealing. The solvent annealing with THF vapor made the final spherical micelles smaller in size as well as more closely packed with each other because of the lower selectivity of THF to PS blocks than that of toluene, as shown

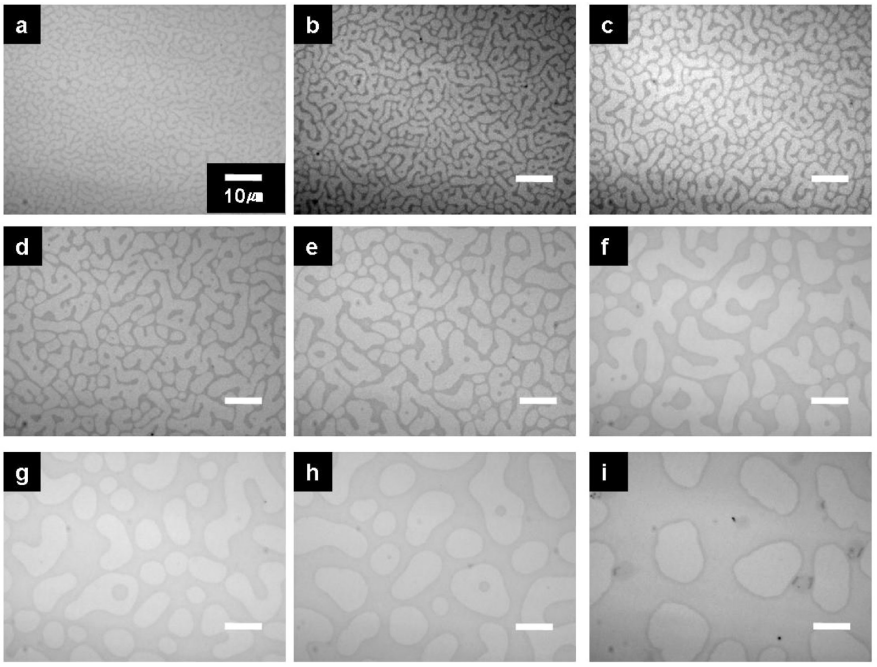

Figure 2. OM images of thin monolayered PS-*b*-P4VP3 micelle films dewetted during solvent annealing with THF vapor. The images were captured of the PS-*b*-P4VP3 micellar film after solvent treated for (a) 10, (b) 20, (c) 30, (d) 40, (e) 60, (f) 80, (g) 100, (h) 150, and (i) 200 min.

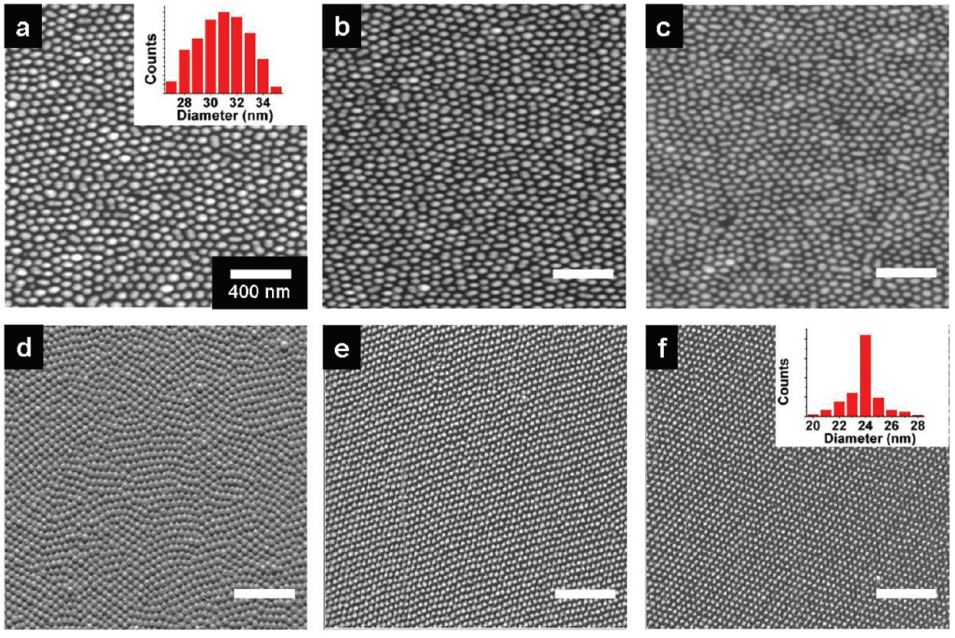

Figure 3. TM-AFM images of (a−c) height and (d−f) phase contrast display morphological evolution of a thin PS-*b*-P4VP1 micelle film during solvent annealing with THF vapor. A monolayered PS-*b*-P4VP micellar film was (a) as-cast and annealed with THF vapor for (b) 5, (c) 20, (d) 60, (e) 90, and (f) 180 min. The insets of parts a and f show size the distribution of the PS-*b*-P4VP1 micelles before and after solvent annealing, respectively.

in Figure 1. The more closed packing of the spherical micelles that are smaller in size may be one of the reasons for dewetting of a film. The previous study by T.P. Russell et al. has also shown that the larger micelles are formed near the dewetting regions by the aggregation of the unstable PS-*b*-P4VP micelles at the dewet regions.[29] It is noteworthy that autophobic dewetting typically developed in a block copolymer film from disordered state and characterized with a thin brush layer[43] did not occur in our micelle film, which implies that our film did not experience the disordered, molten state throughout solvent annealing. It should be also noted that in our system, a wetting layer frequently observed in PS-*b*-P4VP systems in which a polar P4VP layer is strongly bound to a native oxide surface was not formed, even by reducing film thickness, because the spherical micelles in toluene were directly deposited on the substrate.[29] The similar spinodal dewetting also took place with other PS-*b*-P4VP micelle films listed in Table 1.

The pathways to reach the ordered micelle structures of PS-*b*-P4VP1 and PS-*b*-P4VP3 observed in Figure 1c,d, respectively, were investigated with AFM as a function of the solvent annealing time in Figures 3 and 4. In the case of PS-*b*-P4VP1, ordering of micelles is progressively improved with solvent annealing time (Figure 3), and a well-defined ordered micelle structure (Figure 3f) was developed after 3 h of THF treatment. Under our

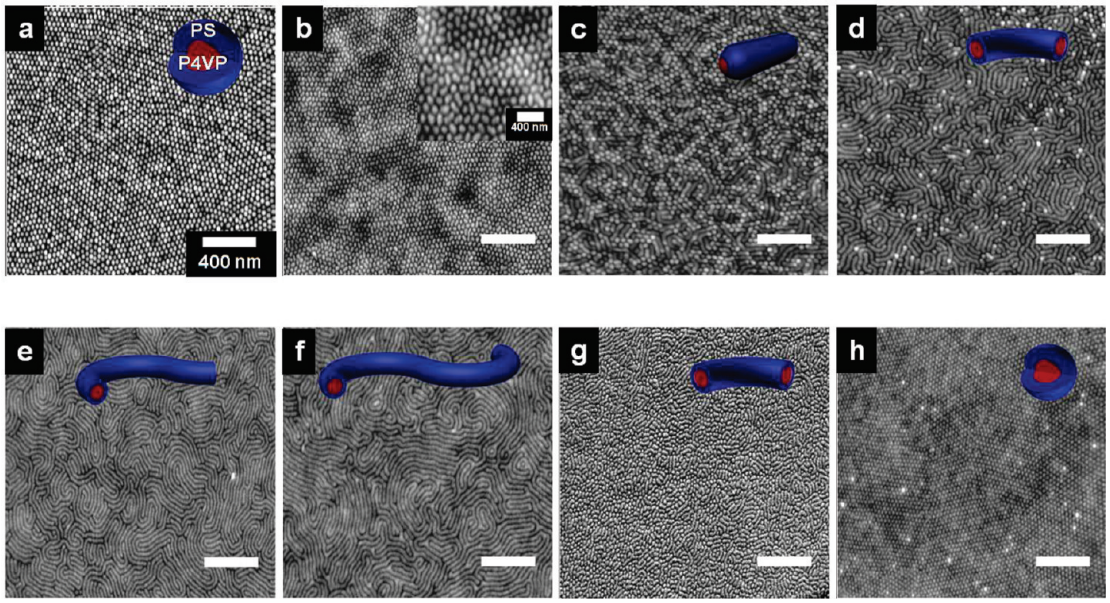

Figure 4. TM-AFM images of (a−d,f) height and (e) phase contrast of morphological evolution of a thin PS-*b*-P4VP3 micelle film during solvent annealing with THF vapor. A thin monolayered film was (a) as-cast and subsequently annealed with solvent vapor for (b) 5, (c) 10, (d) 15, (e) 30, (f) 60, (g) 90, and (h) 180 min. The cylindrical fusion of the initial spherical micelles and subsequent fission into the ordered spherical micelles are apparent. The inset of part b exhibits slightly elongated micelles after 5 min of solvent vapor treatment. The schematics in the Figure represent the micelle structures at different solvent annealing time. One should note that actual micelles in parts a and h on native oxide surface are not spherical, as shown in the schematics.

experimental conditions, where a thin micelle film did not undergo disordered state with block copolymer chains completely molten, the ordered micelle structure arose from the rearrangement and readjustment of the highly mobile as-cast micelles driven by THF solvent vapor. The solvent annealing reduced the averaged core size from approximately 31 to 24 nm. In addition, the micelles become more narrowly distributed in size upon solvent annealing, as clearly shown in the inset of Figure 3f, compared with as-cast micelles (inset of Figure 3a).

When a thin monolayered PS-*b*-P4VP3 micelle film was exposed to THF vapor for a very short time of 5 min, as-cast micelles tended to merge with adjacent ones, leading to ellipsoidal-shaped micelles, as shown in Figure 4b. A magnified image in the inset of Figure 4b clearly exhibits slightly elongated micelles. Longer solvent annealing for 10 min obviously facilitates the fusion process of spherical micelles, giving rise to much longer elongated micelles, as shown in Figure 4c. With further solvent annealing, the elongated micelles turn into cylindrical micelles aligned parallel to the substrate (Figure 4d−f). In particular, the cylindrical micelles locally aligned with each other were observed in a thin film solvent annealed for 60 min in Figure 4f. The presence of the cylindrical micelles with PS coronas after a certain period of time of annealing was again confirmed by XPS, in which carbon electron emission was detected only without the trace of nitrogen electron emission (Figure S3 in the Supporting Information).

Interestingly, the cylindrical micelles began to break themselves into the shorter micelles with further solvent annealing by so-called fission process, as shown in Figure 4g. Further solvent annealing for 3 h lead to a well-ordered spherical micelle structure with uniform micelle size over a large area, as shown in Figure 4h. The ordered spherical structure protruding on the film surface is clearly distinguished from that with P4VP cylinders of a PS-*b*-P4VP copolymer aligned perpendicular to a substrate in which the cylinders are slightly indented from the film surface, as observed in the previous work by Russell et al.[30] In their work, the P4VP cylinders of PS-*b*-P4VP1 aligned perpendicular to a substrate were fabricated by the mixed solvent of toluene and THF and subsequent solvent annealing with THF. Again, the formation of the arrayed spherical micelles with PS coronas was confirmed by XPS, which exhibited no electron emission from nitrogen. Unlike PS-*b*-P4VP1, in which the ordering of spherical micelles arose from the rearrangement and readjustment of the existing spherical micelles, PS-*b*-P4VP3 clearly shows the formation of the ordered micelle structure driven by so-called fusion and fission process.

The fusion of two micelles occurs with sufficient chain mobility when the system overcomes the activation barrier energy, which is on the order of the elastic free energy of the chains associated into a larger micelle.[44] One of the micelles has to penetrate the dense corona region of the other micelle. Micellar fission starts with the separation of micellar cores, which increases the total surface free energy corresponding to the activation energy for fission. The subsequent corona separation decreases the total free energy through entropy gain for the micelles. In the real system, both fusion and fission strongly depend on kinetics of structure evolution characterized by various diffusion times for micelle merge and separation.[44,45] The theoretical studies show that the rates of micelle fusion and fission are mainly determined by the characteristic micelle diffusion time and corona deformation time. Both times are scaled by $\sim N^{x}_{\mathrm{corona}}$, where N_{corona} corresponds to the corona length and x is index greater than one, which indicates that the diffusion time increases with an increase in the length and concentration of corona block.

The initial spherical micelles of PS-*b*-P4VP3 formed in toluene are kinetically trapped on a Si substrate by the fast spin-coating process and are subject to transform their structures into ones thermodynamically in equilibrium determined by the relative block length of two constituent ones when copolymer chains become mobile. In our system, THF provides the sufficient mobility of both blocks upon exposure of its vapor because it is a good solvent for both PS and P4VP blocks but is slightly preferential to the PS block.[12] The solvent annealing begins to drive the spherical micelles eventually into lamellae morphology by initiating the fusion of spherical

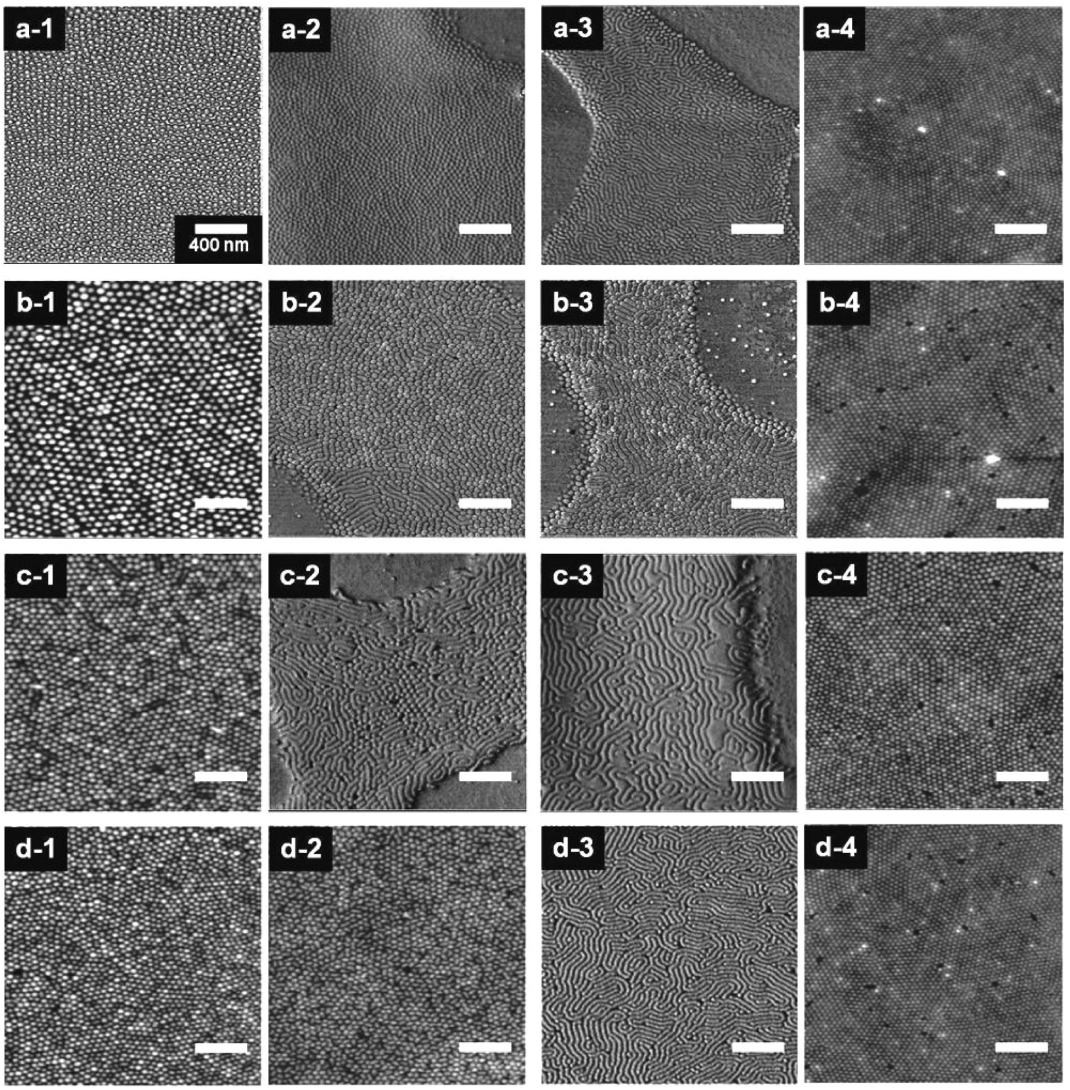

Figure 5. Morphological evolutions of (a) PS-*b*-P4VP2, (b) PS-*b*-P4VP4, (c) PS-*b*-P4VP5, and (d) PS-*b*-P4VP6 micelle films during solvent annealing with THF vapor. The numbers 1, 2, 3, and 4 in a row correspond to as-cast and solvent annealing times of 15, 30, and 180 min, respectively.

micelles into cylindrical micelles, as evidenced in Figure 4a−d. The thin film morphology would not, however, reach the equilibrium lamellae structure in our experiments because of the preferentiality of THF to PS blocks, which makes the effective volume fraction of PS larger and larger with solvent annealing time. The system now tends to transform the cylindrical micelles into spherical micelles again by fission process, as observed in Figure 4e,f. The fission process rendered the individual spherical micelles smaller and more regular in size, leading to the highly ordered micelle packing, as not only observed in Figure 4h but also consistent with the previous results.[12] On the basis of our experimental results and understanding, we believe that the structure transition from sphere to cylinder to sphere resulted from the thermodynamic pathway of the material system including solvent rather than solvent specifics. It is, therefore, plausible, in principle, to obtain different structures if the concentration of THF is properly controlled. For instance the P4VP cylinders ordered parallel to the substrate can be stabilized at lower THF concentration, although we have not succeeded in stabilizing the cylinder structure because of the difficulty in controlling the solvent concentration in our experimental setup. The easier way to obtain a transient structure is to control the time interval of solvent annealing, as shown later.

The structure transformation in the late stage of solvent annealing from cylinder to sphere is also related to the increased effective volume fraction of PS domains (where the solvent molecules are selectively absorbed) during solvent annealing, which is a purely thermodynamic argument that the final destination of the solvent-annealed block copolymer is the spherical mesophase in this experimental setup. In this situation, there may be an argument as to why the as-cast, larger spherical micelle has to pass through cylinders to get the smaller sphere as the final destination, which is seemingly counterintuitive because large micelles can simply expel chains to form smaller micelles and do not necessarily transit to cylinders. However, we suppose that this counterintuitive sphere-to-cylinder transformation in the initial stage of solvent annealing is attributed to the packing density difference between core and corona in the as-cast micelles. In the early stage of solvent annealing, the initial as-cast micelle is expected to consist of a densely packed 4 VP core and loosely packed PS domains (because of rapid solvent evaporation) and tends to level the density difference as the initially frozen chains start to move because of solvent annealing. One of possibilities for the leveling density difference between the core and the corona region is the reducing curvature of the interface (in view of the core side) in either an isotropic way (larger sphere or plane) or an anisotropic way (cylinder). Of course, without any quantitative

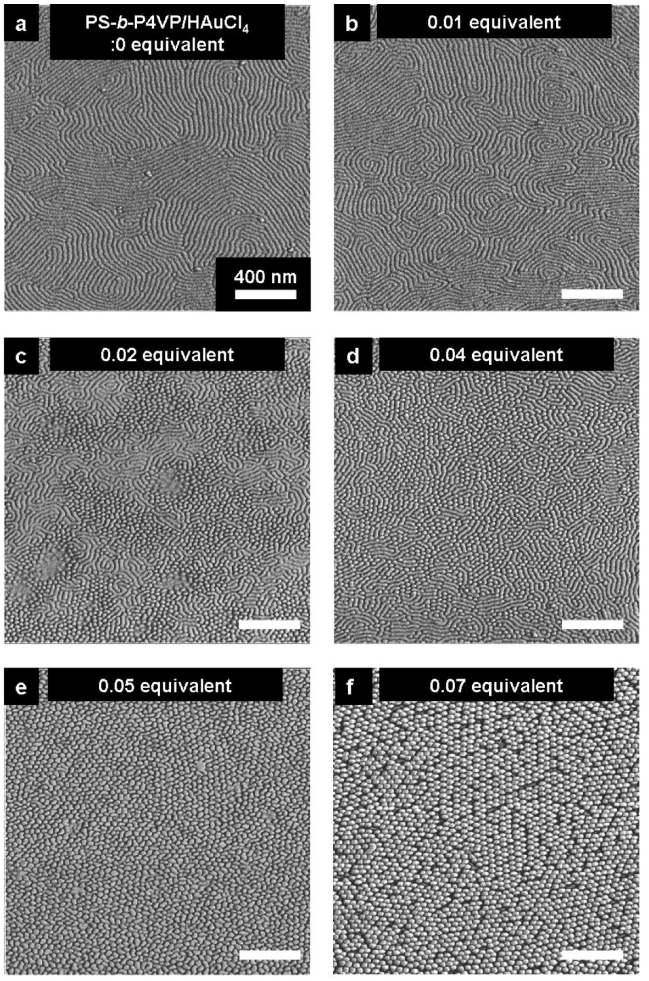

Figure 6. TM-AFM images in phase contrast of thin PS-*b*-P4VP3 micelle films exposed to THF vapor for 1 h with different amount of $HAuCl_4$ ranging from (a) 0, (b) 0.01, (c) 0.02, (d) 0.04, (e) 0.05, to (f) 0.07 with respect to P4VP block. The formation of the fused cylindrical micelles is significantly delayed because of the strong coordination of $HAuCl_4$ to P4VP, which in turn hinders the diffusion of P4VP block.

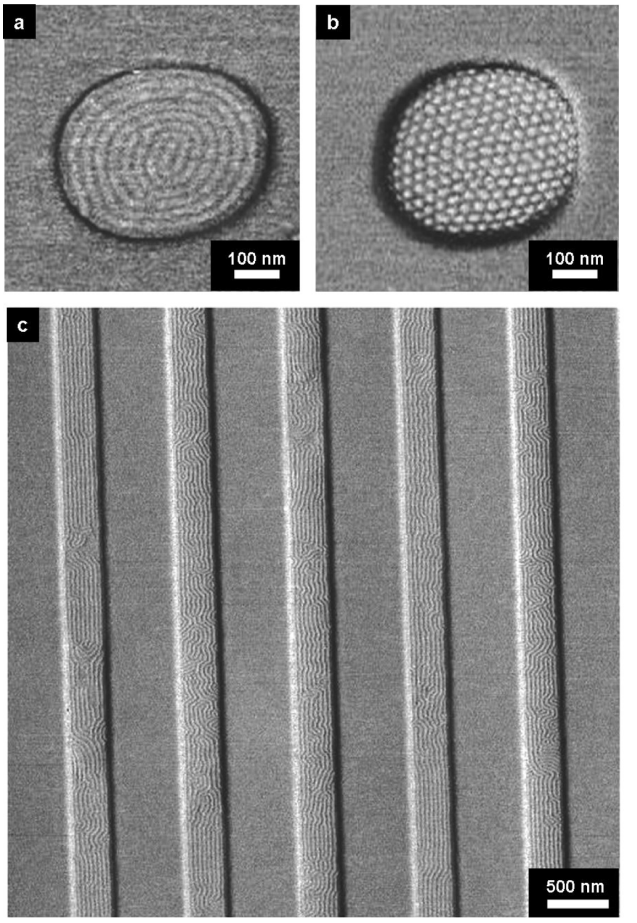

Figure 7. TM-AFM images in phase contrast of PS-*b*-P4VP3 films confined in topographic prepatterns. Solvent annealing of a micelle film confined in a circular dent for (a) 60 and (b) 180 min produces well-defined concentric cylindrical and closely packed spherical micelles, respectively. (c) Cylindrical PS-*b*-P4VP micelles are also confined and well-aligned along periodic trenches after THF solvent annealing for 60 min.

information (initial density difference, time-dependent amount of solvents absorbed in the film, etc.), it is not straightforward to conclude that such curvature change for leveling density difference should result in cylindrical shape in the early stage of solvent annealing, but it is very unlikely that as-cast larger micelles transform directly to smaller micelles simply by expelling some chains.

PS-*b*-P4VP1 with the longest corona PS block among our block copolymers (Table 1) hardly undergoes the fusion and fission process during solvent annealing because of very long micelle diffusion and deformation times and thus forms an ordered micelle structure by the rearrangement of the initial spherical micelles similar to the assembly of hard sphere colloids. It is likely that the unimer exchange process partially contributes to the spherical micelle reorganization of PS-*b*-P4VP1, although we do not have any experimental evidence. Many theories predict that the unimer exchange process can be dominant for micelle reorganization in a solvent swollen film because of its low energy barrier.[46,47] On the contrary, the micelles of PS-*b*-P4VP3 with the relatively short PS block easily overcome the activation barriers for fusion and fission, which consequently leads to the ordered micelles upon solvent annealing. To confirm our speculation, we also employed the different block copolymers listed in Table 1. All PS-*b*-P4VP copolymers (2, 4, 5, and 6 in Table 1) with the PS corona block similar or shorter than that of PS-*b*-P4VP3 undergo fusion and fission of the initial spherical micelles to reach ordered spherical micelle arrays upon solvent annealing for 3 h, as shown in Figure 5. It should be noted that similar to PS-*b*-P4VP3, the microstructure evolution of all block copolymers occurred simultaneously with dewetting of the thin films. Additional experimental caution should be made to ensure that a monolayered film of the spherical micelles is initially obtained because cylindrical micelles of a PS-*b*-P4VP copolymer are often formed in solution depending on the solution temperature. In fact, for PS-*b*-P4VP1, the cylindrical micelles are frequently formed when a solution is prepared at a temperature below 60 °C. At high temperature above 60 °C, the cylindrical micelles become spherical micelles. To avoid the fission and fusion in the solution state, our solutions were all prepared at 80 °C and immediately spin coated on a substrate. The monolayered spherical micelles were always confirmed before solvent annealing.

To control the kinetics of fusion and fission of the spherical micelles, we selectively incorporated a metallic salt, $HAuCl_4$, into the P4VP cores of PS-*b*-P4VP3 micelles. The strong coordination of $HAuCl_4$ in polar P4VP blocks arises from the lone pair electrons in pyridine units of P4VP blocks that are easily protonated with $AuCl_4^-$ ions and thus significantly hinders the chain diffusion in the cores. Our experimental data indeed show that the spherical-to-cylindrical micelle fusion was greatly delayed

with $HAuCl_4$ added to block copolymer micelles in Figure 6. The samples with a different amount of $HAuCl_4$ with respect to P4VP blocks were equally treated with THF vapor for 1 h. Whereas relatively long cylindrical micelles are fully developed without the metallic salt added (Figure 6a), almost no cylindrical micelles are observed with 0.07 equiv $HAuCl_4$ with respect to P4VP blocks as shown in Figure 6f. It is also apparent from Figure 6b−e that the population of the fused cylindrical micelles decreases with $HAuCl_4$. In addition, further solvent annealing of the sample with 0.07 equiv $HAuCl_4$ for more than 3 h resulted in spherical micelles closely packed without their long-range ordering, similar to the as-cast micelles shown in Figure 1b. The results indirectly confirm that the long-range ordering of the spherical micelles of PS-*b*-P4VP3 was driven through the fusion and subsequent fission of the micelles.

Our experimental observations with PS-*b*-P4VP copolymers involving the fusion and fission of the micelles also suggest that in principle one can intentionally utilize one of the microstructures kinetically evolved during solvent annealing by controlling the solvent annealing time. For instance, we employed a topographic prepattern for controlling both microstructure and the lateral orientation of a PS-*b*-P4VP3 upon solvent annealing. We purposely developed the fused cylindrical micelles confined in a circular dent by controlling the solvent annealing time. A variety of the confined cylindrical structures were observed with the packing defects, and in some cases, a circular dent was fully covered by concentric PS-*b*-P4VP3 cylinders, as shown in Figure 7a. The fission of the cylindrical micelles of the PS-*b*-P4VP3 film in the prepattern occurred upon further solvent annealing, leading to the ordered spherical micelles graphoepitaxially confined in a circular dent, as shown in Figure 7b. In addition, as-cast spherical PS-*b*-P4VP3 micelles on topographically patterned periodic lines were fully transformed into cylindrical ones by the micelle fusion with solvent vapor and aligned along the line direction with some structural defects in Figure 7c. We are currently investigating the structure evolution on the patterned substrates as a function of trench width and depth for future work.

Conclusions

We examined the structural evolution of monolayered spherical micelle films of various PS-*b*-P4VP copolymers with different block lengths and compositions upon THF solvent annealing. Depending on the molecular weight of the PS corona block, two different kinetic pathways were observed to reach the spherical micelle arrays hexagonally packed with a long-range order. For PS-*b*-P4VP1 with 47 000 g/mol PS blocks, the ordered structure arose from the rearrangement and readjustment of the initial spherical micelles. However, in the case of PS-*b*-P4VP copolymers with PS blocks ranging from approximately 10 000 to 20 000 g/mol, the ordered structures of spherical micelles were driven through fusion and subsequent fission of the initial spherical micelles. The fusion of the spherical micelles to cylindrical micelles was kinetically controlled by the addition of $HAuCl_4$, which coordinated itself selectively with the polar P4VP blocks and consequently hindered the diffusion of the P4VP chain upon solvent vapor exposure. Furthermore, the delicate control of the fusion and fission of the micelles by solvent annealing time enabled us to fabricate well-ordered cylindrical or spherical microstructures graphoepitaxially confined into the topographically patterned substrates.

Acknowledgment. This work was supported by DAPA and ADD, the Korea Research Foundation Grant funded by the Korean Government. (MOEHRD; KRF-2005-042-D00110), Korea Ministry of Knowledge and Economy through the project of NGNT (no. 10024135-2005-11) and Seoul Research and Business Development Program (10701). The X-ray experiments at PAL (4C2 beamline), Korea, were supported by MEST and POSCO, Korea. This work was supported by the Second Stage of the Brain Korea 21 Project in 2006 and by the Seoul Science Fellowship.

Supporting Information Available: 2D GISAXS image of an as-cast monolayered PS-*b*-P4VP3 film and XPS spectra of a thin micelle film of PS-*b*-P4VP3 treated with ethanol and THF vapors. This material is available free of charge via the Internet at http://pubs.acs.org.

References and Notes

(1) Hamley, I. W. *Angew. Chem., Int. Ed.* **2003**, *42*, 1692.
(2) Park, C.; Yoon, J.; Thomas, E. L. *Polymer* **2003**, *44*, 6725.
(3) Hamley, I. W. *The Physics of Block Copolymers*; Oxford University Press: Oxford, U.K., 1998
(4) Meiners, J. C.; Quintel-Ritzi, A.; Mlynek, J.; Elbs, H.; Krausch, G. *Macromolecules* **1997**, *30*, 4945.
(5) Krupers, M. J.; Sheiko, S. S.; Möller, M. *Polym. Bull.* **1998**, *40*, 211.
(6) Wen, G.; Chung, B.; Chang, T. *Polymer* **2006**, *47*, 8575.
(7) Korczagin, I.; Hempenius, M. A.; Fokkink, R. G.; Cohen Stuart, M. A.; Al-Hussein, M.; Bomans, P. H. H.; Frederik, P. M.; Julius Vancso, G. *Macromolecules* **2006**, *39*, 2306.
(8) Yun, S.-H.; Sohn, B.-H.; Jung, J. C.; Zin, W.-C.; Ree, M.; Park, J. W. *Nanotechnology* **2006**, *17*, 450.
(9) Segalman, R. A.; Hexemer, A.; Hayward, R. C.; Kramer, E. J. *Macromolecules* **2003**, *36*, 3272.
(10) Vedrine, J.; Hong, Y.-R.; Marencic, A. P.; Register, R. A.; Adamson, D. H.; Chaikin, P. M. *Appl. Phys. Lett.* **2007**, *91*, 143110.
(11) Cheng, J. Y; Zhang, F.; Chuang, V. P.; Mayes, A. M.; Ross, C. A. *Nano Lett.* **2006**, *6*, 2099.
(12) Yun, S. H.; Yoo, S. I.; Jung, J. C.; Zin, W. C.; Sohn, B. H. *Chem. Mater.* **2006**, *18*, 5646.
(13) Angelescu, D. E.; Waller, J. H.; Register, R. A.; Chaikin, P. M. *Adv. Mater.* **2005**, *17*, 1878.
(14) Hahn, J.; Webber, S. E. *Langmuir* **2003**, *19*, 3098.
(15) Hahn, J.; Webber, S. E. *Langmuir* **2004**, *20*, 1489.
(16) Hahn, J.; Webber, S. E. *Langmuir* **2004**, *20*, 4211.
(17) Lin, X. M.; Jaeger, H. M.; Sorensen, C. M.; Klabundem, K. J. *J. Phys. Chem. B* **2001**, *105*, 3353.
(18) Narayanan, S.; Wang, J.; Lin, X.-M. *Phys. Rev. Lett.* **2004**, *93*, 135503.
(19) Fu, Y.; Jin, Z.; Liu, Z.; Liu, Y.; Li, W. *Mater. Lett.* **2008**, *62*, 4286.
(20) Kim, S. H.; Minsner, M.; Xu, T.; Kimura, M.; Russell, T. P. *Adv. Mater.* **2004**, *16*, 226.
(21) Fukunaga, K.; Hashimoto, T.; Elbs, H.; Krausch, G. *Macromolecules* **2002**, *35*, 4406.
(22) Ludwigs, S.; Böker, A.; Voronov, A.; Rehse, N.; Magerle, R.; Krausch, G. *Nat. Mater.* **2003**, *2*, 744.
(23) Cavicchi, K. A.; Berthiaume, K. J.; Russell, T. P. *Polymer* **2005**, *46*, 11635.
(24) Bang, J.; Kim, S. H.; Drockenmuller, E.; Misner, M. J.; Russell, T. P.; Hawker, C. J. *J. Am. Chem. Soc.* **2006**, *128*, 7622.
(25) Cavicchi, K. A.; Russell, T. P. *Macromolecules* **2007**, *40*, 1181.
(26) Hwang, J.; Huh, J.; Jung, B.; Hong, J. M.; Park, M.; Park, C. *Polymer* **2005**, *46*, 9133.
(27) Kim, T. H.; Hwang, J.; Hwang, W. S.; Huh, J.; Kim, H.-C.; Kim, S. H.; Hong, J. M.; Thomas, E. L.; Park, C. *Adv. Mater.* **2008**, *20*, 522.
(28) Zhao, J.; Jiang, S.; Ji, X.; An, L.; Jiang, B. *Polymer* **2005**, *46*, 6513.
(29) Park, S.; Kim, B.; Yavuzcetin, O.; Tuominen, M. T.; Russell, T. P. *ACS Nano* **2008**, *2*, 1363.
(30) Park, S.; Kim, B.; Xu, J.; Hofmann, T.; Ocko, B. M.; Russell, T. P. *Macromolecules* **2009**, *42*, 1278.
(31) Kim, B.; Park, S.; McCarthy, T. J.; Russell, T. P. *Small* **2007**, *3*, 1869.
(32) Park, S.; Wang, J.-Y.; Kim, B.; Chen, W.; Russell, T. P. *Macromolecules* **2007**, *40*, 9059.
(33) Hanley, K. J.; Lodge, T. P.; Huang, C.-I. *Macromolecules* **2000**, *33*, 5918.
(34) Peng, J.; Xuan, Y.; Wang, H.; Yang, Y.; Li, B.; Han, Y. *J. Chem. Phys.* **2004**, *120*, 11163.
(35) Xuan, Y.; Peng, J.; Cui, L.; Wang, H.; Li, B.; Han, Y. *Macromolecules* **2004**, *37*, 7301.

(36) Li, X.; Peng, J.; Wen, Y.; Kim, D. H.; Knoll, W. *Polymer* **2007**, *48*, 2434.
(37) Yoo, S. I.; Sohn, B. H.; Zin, W. C.; Jung, J. C.; Park, C. *Macromolecules* **2007**, *40*, 8323.
(38) Förster, S.; Zisenis, M.; Wenz, E.; Antonietti, M. *J. Chem. Phys.* **1996**, *104*, 9956.
(39) Herminghaus, S.; Jacobs, K.; Mecke, K.; Bischof, J.; Fery, A.; Ibn-Elhaj, M.; Schlagowski, S. *Science* **1998**, *282*, 916.
(40) Xie, R.; Karim, A.; Douglas, J. F.; Han, C. C.; Weiss, R. A. *Phys. Rev. Lett.* **1998**, *81*, 1251.
(41) Higgins, A. M.; Jones, R. A. L. *Nature* **2000**, *404*, 476.
(42) Seemann, R.; Herminghaus, S.; Jacobs, K. *J. Phys.: Condens. Matter* **2001**, *13*, 4925.
(43) Limary, R.; Green, P. F. *Macromolecules* **1999**, *32*, 8167.
(44) Dormidontova, E. E. *Macromolecules* **1999**, *32*, 7630.
(45) Esselink, F. J.; Dormidontova, E. E; Hadziioannou, G. *Macromolecules* **1998**, *31*, 2925.
(46) Creutz, S.; Van Stam, J.; De Schryver, F. C.; Jérome, R. *Macromolecules* **1998**, *31*, 681.
(47) Colombani, O.; Ruppel, M.; Schubert, F.; Zettl, H.; Pergushov, D. V.; Muller, A. H. E. *Macromolecules* **2007**, *40*, 4338.